

Synthesis and electrochemical performance of $\text{Fe}_2(\text{MoO}_4)_3$ cathode for sodium-ion batteries

Nguyen Van Tu^{1,2*}, Phan Quang Quy³

¹State Key Laboratory of Advanced Technology for Materials Synthesis and Processing, School of Material Science and Engineering, Wuhan University of Technology, Wuhan 430070, P. R. China

²Institute for Chemistry and Materials, Military Institute of Science and Technology

³Hanoi University of Industry

Received 29 January 2016; Accepted 12 August 2016

Abstract

In this articles, $\text{Fe}_2(\text{MoO}_4)_3$ was prepared by precipitation method and used as cathode materials for sodium-ion batteries. The crystalline structure of the sample was characterized by a powder X-ray diffraction spectroscopy (XRD), the morphologies of the sample were observed by the field emission scanning electron microscopy (SEM), the binding state of elements in sample was analyzed by X-ray photoelectron spectroscopy (XPS). The electrochemical properties were investigated in CR2025 coin type cell with a metal sodium foil as the anode electrode. As the charge/discharge current density at 0.1 C, the initial specific capacity of $\text{Fe}_2(\text{MoO}_4)_3$ is 82.50 mAhg^{-1} , and remains 67.92 mAhg^{-1} after 15 cycles.

Keywords. NASICON, iron molybdate, sodium ion battery, cathode material.

1. INTRODUCTION

Sodium-ion batteries (SIBs) are the most promising alternatives to lithium-ion batteries due to the low cost and abundance of sodium element in the earth. The chemical similarity of sodium ion toward lithium ion enables some electrode materials used in Li-ion batteries (LIBs) to be applied for SIBs. Specialty for the application in the large-scale energy storage for smart grid and solar/wind energy, and the problem of low-cost would be a big challenge [1].

Since the 1980s, many cathode materials for sodium-ion battery have been identified, such as Na_xMO_2 [2], NaFePO_4 [3], MF_3 [4], NaMnPO_4 [5], $\text{Na}_2\text{MPO}_4\text{F}$ [6], $\text{Na}_3\text{M}_2(\text{PO}_4)_3\text{F}$ [7] ($\text{M} = \text{Fe}, \text{V}, \text{Mn}$), V_2O_5 [8], $\text{Na}_3\text{V}_2(\text{PO}_4)_3$ [9], NASICON (Na^+ superionic conductor) compounds, and organic compounds [10]. But the limitations of the material are the insertion/extraction of Na^+ ions which is difficult, due to large size of Na^+ (1.02 \AA). It is a big challenge for the research community to find suitable cathode materials, which can be used in sodium-ion batteries.

Though Na^+ ion has larger ionic size, the insertion/extraction of it is easy and fast in the structure of NASICON compounds due to the 3D

structure of $\text{Fe}_2(\text{MoO}_4)_3$. NASICON- $\text{Fe}_2(\text{MoO}_4)_3$ has been identified as a potential candidate for sodium storage due to the low price, non-toxicity of iron and its open three dimensions framework. However, its poor cycle-ability and low electric conductivity limit its further applications [11].

In this paper there have been studied the preparation, characterization and electrochemical properties of four $\text{Fe}_2(\text{MoO}_4)_3$ samples. The relativity between structure and properties are also analyzed. A reasonable explanation for the mechanism to improve the electrochemical performance is given in our work.

2. EXPERIMENTAL

2.1. Synthesis $\text{Fe}_2(\text{MoO}_4)_3$ powder

Monoclinic $\text{Fe}_2(\text{MoO}_4)_3$ powder was synthesized by a precipitation method described elsewhere [2]. $0.983 \text{ g } (\text{NH}_4)_6\text{Mo}_7\text{O}_{24}\cdot 4\text{H}_2\text{O}$ was dissolved in 20 mL distilled water, referring as solution A. $1 \text{ g } \text{Fe}(\text{NO}_3)_3\cdot 9\text{H}_2\text{O}$ was dissolved in 20 mL distilled water, referring as solution B. Then the solution B was slowly added to solution A under continuous stirring and HNO_3 was added to adjust the pH value to 2, 3, 4 and 5. Later, the obtained solution was

heated to 95-100 °C for 2 hours. Finally, the precipitate was then aged, filtered, washed and calcined at 500-650 °C in air for 25 hours. The sample was allowed to cool in furnace till room temperature.

2.2. Characterization

The crystalline structure of the sample was characterized by a powder X-ray diffraction spectroscopy (XRD, PertrPro PANalytical, Netherlands) equipped with $\text{CuK}\alpha$ radiation (1.5418 Å). The morphologies of the sample were observed by the field emission scanning electron microscopy (SEM, JSM-6700F, JEOL, Tokyo, Japan). X-ray photoelectron spectroscopy (XPS) measurements were acquired using a VG Multilab 2000, with $\text{AlK}\alpha$ the as the radiation source. All XPS spectra were corrected by the C1s line at 284.8 eV.

The electrochemical properties were investigated in CR2025 coin type cell with a metal sodium foil as the anode electrode. The NaClO_4 (Aldrich, 99.99 wt%) and the solvent propylene carbonate were used as an electrolyte (1 mol/L). The working electrode was prepared by spreading the slurry of the $\text{Fe}_2(\text{MoO}_4)_3$ (80 wt%), acetylene black (15 wt%), and binder polytetrafluoroethylene (PTFE) (5wt%) on Ni mesh. Polypropylene microporous film (Cellgard 2300) is used as a separator. The cells were assembled in an argon-filled glove box at room temperature. For galvanostatic charge-discharge test were carried out on a battery test system (Land BT2000, Wuhan, China). The cyclic voltammetry (CV) and electrochemical impedance spectroscopy (EIS) were measured by Autolab Potentiostat 30.

3. RESULTS AND DISCUSSION

3.1. Morphology and structure

XRD patterns of the samples are shown in figure 1. It can be observed that the peaks are well indexed of monoclinic structure of $\text{Fe}_2(\text{MoO}_4)_3$ (JCPDS 01-072-0935), as impurities of MoO_3 , Fe_3O_4 . XRD patterns of $\text{Fe}_2(\text{MoO}_4)_3$ were successfully indexed with a monoclinic lattice using the program Jade 6.5. The unit cell lattice parameters of all the experimental $\text{Fe}_2(\text{MoO}_4)_3$ phases are summarized in table 1. On the table 1, the lattice parameters changed little with different pH values of conditional preparation. The results of XRD analysis indicate $\text{Fe}_2(\text{MoO}_4)_3$ sample prepared at pH = 4 is pure than every samples.

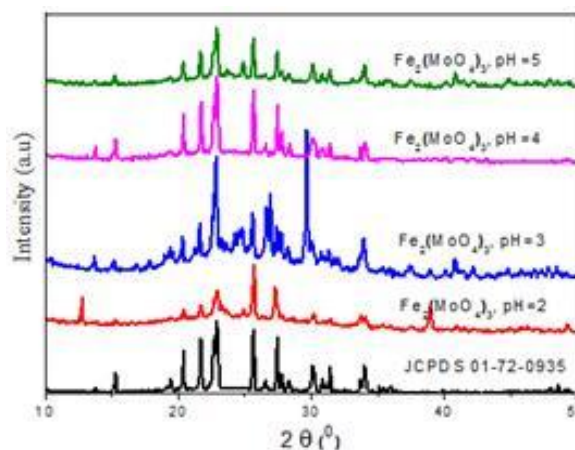


Figure 1: XRD patterns of the samples at different pH values and pure $\text{Fe}_2(\text{MoO}_4)_3$ (JCPDS 01-072-0935)

Table 1: Refined unit cell lattice parameters for $\text{Fe}_2(\text{MoO}_4)_3$ cell at different pH values

| pH | a(Å) | b(Å) | c(Å) | β (°) | V(Å ³) |
|----|---------|--------|---------|-------------|--------------------|
| 2 | 15.7251 | 9.1971 | 18.2505 | 125.529 | 2148.98 |
| 3 | 15.7272 | 9.1970 | 18.2520 | 125.532 | 2150.89 |
| 4 | 15.7266 | 9.1967 | 18.2514 | 125.539 | 2148.04 |
| 5 | 15.7271 | 9.1969 | 18.2498 | 125.452 | 2147.97 |

The SEM images of $\text{Fe}_2(\text{MoO}_4)_3$ samples at different pH values are shown in figure 2. It can be observed that the particles are uniform and fine sizes. Particle sizes are about 0.2-1 μm and the particle sizes are observed to be smaller at lower pH. This issue may be explained by precipitation of MoO_3 at lower pH value. From results of XRD and SEM analysis, we select synthetic condition of $\text{Fe}_2(\text{MoO}_4)_3$ at pH = 4 for all experiments.

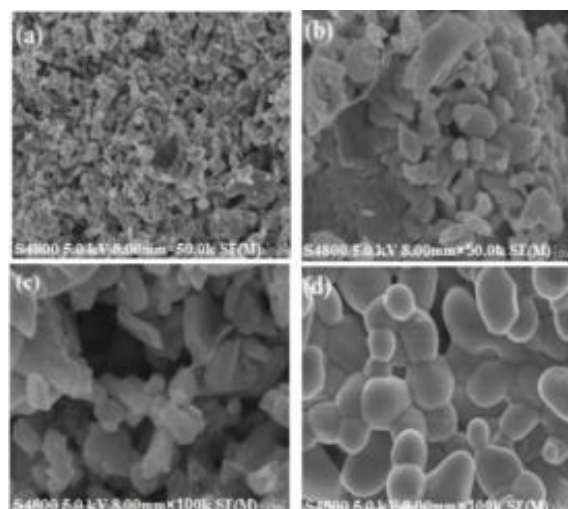


Figure 2: SEM images of $\text{Fe}_2(\text{MoO}_4)_3$ samples. (a) pH = 5, (b) pH = 4, (c) pH = 3, (d) pH = 2

The formation of $\text{Fe}_2(\text{MoO}_4)_3$ is further investigated using X-ray photoelectron spectroscopy (XPS). It is well known that the electrochemical properties of the sample are related with their sizes and phases as well as their chemical binding states. The XPS survey spectra in figure 3a show that Fe, Mo, and O elements coexist. Further, the spectra of Fe2p and Mo3d in figure 3c and figure 3d show the characteristic peaks of Fe^{3+} state and Mo^{6+} state located at 711.79 eV and 232.8 eV, respectively (the states of Fe^{3+} and Mo^{6+} in $\text{Fe}_2(\text{MoO}_4)_3$).

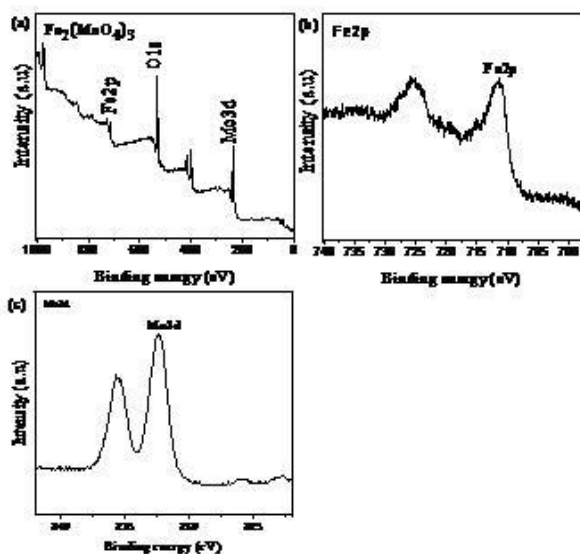
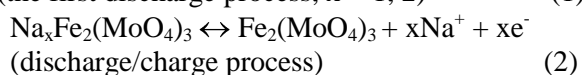
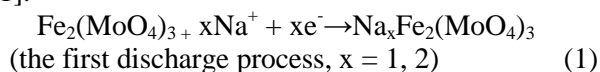


Figure 3: X-ray photoelectron spectra of $\text{Fe}_2(\text{MoO}_4)_3$ powder (a) Survey spectra; (b) Fe2p spectra, (c) Mo3d spectra

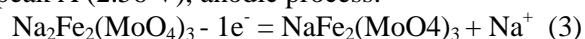
3.2. Electrochemical performances and reaction mechanism

The cyclic voltammetry curves of the $\text{Fe}_2(\text{MoO}_4)_3$ between 1.5 and 3.5 V at a scan rate of 0.1 mV s^{-1} are shown in figure 4a. Two cathodic current peaks at 2.61 and 2.52 V are observed in the first reduction process and shifted to 2.62 V and 2.53 V in the subsequent ones. During all oxidation processes, there are two corresponding anodic peaks at 2.56 and 2.71 V. The intensities of peaks are well maintained in all subsequent cycles. The results are in a good agreement with the galvanostatic cycling profiles and indicate a reversible two-step electrochemical reaction mechanism of $\text{Fe}_2(\text{MoO}_4)_3$ with sodium. This result is consistent with our previous report, and it can be expressed as follows [11].



On the figure 4a, the oxidation/reduction reactions between $\text{Fe}_2(\text{MoO}_4)_3$ and $\text{Na}_x\text{Fe}_2(\text{MoO}_4)_3$ are shown as follow:

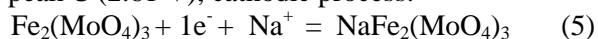
At peak A (2.56 V), anodic process:



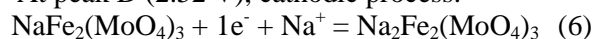
At peak B (2.71 V), anodic process:



At peak C (2.61 V), cathodic process:



At peak D (2.52 V), cathodic process:



These results clearly reveal that the insertion/extraction of Na^+ ions occur inside $\text{Fe}_2(\text{MoO}_4)_3$.

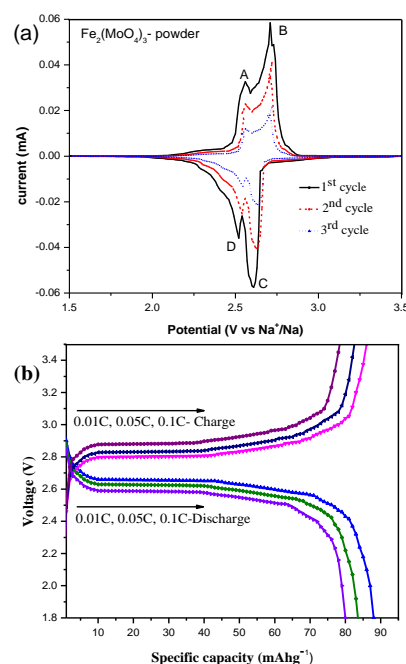


Figure 4: (a) The first cyclic voltammetry curves of $\text{Fe}_2(\text{MoO}_4)_3$ powder electrode at a voltage sweep rate of 0.1 mVs^{-1} , (b) Galvanostatic curves of $\text{Fe}_2(\text{MoO}_4)_3/\text{Na}$ cell at a current rate of 0.1 C

Figure 4b shows the first charge/discharge profiles of $\text{Fe}_2(\text{MoO}_4)_3/\text{Na}$ cell at a current rates of 0.01, 0.05, 0.1 C. The open circuit voltage (OCV) of $\text{Fe}_2(\text{MoO}_4)_3/\text{Na}$ cell is 2.72 V. The discharge capacities of $\text{Fe}_2(\text{MoO}_4)_3$ at 0.1 C is about 82.6 mAh/g and 81.8 mAh/g, respectively, corresponding to about 2.0 Na^+ per formula unit (p.f.u), which means completely transformed the Fe^{3+} to Fe^{2+} .

Figure 4c clearly shows that the $\text{Fe}_2(\text{MoO}_4)_3$ electrode may be the charge/discharge at 0.1 C, the initial specific capacity of $\text{Fe}_2(\text{MoO}_4)_3$ is 82.5 mAh/g, and remains 67.92 mAh/g after 15 cycles.

Figure 4d shows the Nyquist plots of $\text{Fe}_2(\text{MoO}_4)_3$ cathode after 3 cycles at 9 mA/g in the frequency range between 100 kHz and 0.1 Hz at

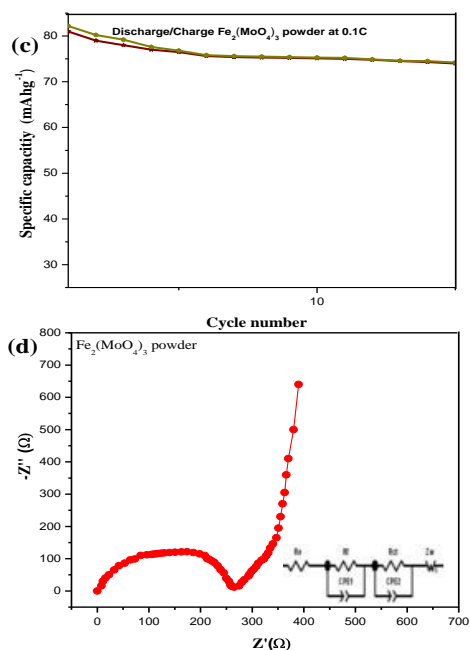


Figure 4 (c): The specific capacities of $\text{Fe}_2(\text{MoO}_4)_3$ powder at 0.1 C (Electrolyte is 1 M NaClO_4 in propylene carbonate (PC)), (d) EIS plots of $\text{Fe}_2(\text{MoO}_4)_3$ powder after 3 cycles at 9 mA/g in the frequency range between 100 kHz and 0.1 Hz at open circuit voltage (OCV) with 5 mV amplitude voltage (Inset shows the equivalent circuits corresponding to the Nyquist plots)

open circuit voltage (OCV) with 5 mV amplitude voltage. The semicircles at high to medium frequency are mainly related to a complex reaction process at the electrolyte/cathode interface. The inclined line in the lower frequency region is

attributed to the Warburg impedance, which is associated with sodium-ion diffusion in the $\text{Fe}_2(\text{MoO}_4)_3$ electrode. The impedance spectra fitted using an equivalent circuit in which R_e represents the total resistance of electrolyte, electrode and separator; R_f and CPE1 are related to the diffusion resistance of Na-ions through the solid electrolyte interface (SEI) layer and the corresponding constant phase element (CPE); R_{ct} and CPE2 correspond to the charge transfer resistance and the corresponding CPE; Z_w is Warburg impedance [12]. The exchange current density is calculated using the following equation.

$$i^0 = RT/nFR_{ct} \quad (7)$$

The fitting results of R_e , R_f , R_{ct} and i^0 as shown in table 2 indicate that the R_f and R_{ct} values of $\text{Fe}_2(\text{MoO}_4)_3$ cathode are big. It can be confirmed that the decrease of charge transfer resistance is beneficial to the kinetic behaviors during charge/discharge process. Since the $\text{Fe}_2(\text{MoO}_4)_3$ shows big resistance and the small exchange current density, it is suggested that $\text{Fe}_2(\text{MoO}_4)_3$ powder significantly unimproved the performance of the sodium-ion battery.

4. CONCLUSION

$\text{Fe}_2(\text{MoO}_4)_3$ was prepared by precipitation method and used materials cathode for sodium-ion batteries. For the technological condition, the $\text{Fe}_2(\text{MoO}_4)_3$ electrode may be the charge/discharge at 0.1 C, the initial specific capacity of $\text{Fe}_2(\text{MoO}_4)_3$ is 82.5 mAh/g, and remains 67.92 mAh/g after 15 cycles. Synthesis of $\text{Fe}_2(\text{MoO}_4)_3$ samples may be used for material cathode for sodium-ion batteries.

Table 2: Impedance parameters calculated from equivalent circuits

| Sample | R_e (Ω) | R_f (Ω) | R_{ct} (Ω) | i^0 (mAcm^{-2}) |
|---|--------------------|--------------------|-----------------------|------------------------------|
| $\text{Fe}_2(\text{MoO}_4)_3$ powder (pH = 4) | 10.55 | 120.86 | 265.60 | 4.831×10^{-5} |

REFERENCES

- Komaba S, Yabuuchi N, Kubota K, et al. *Research development on sodium-ion batteries*, Chemical Reviews, **114**, 11636-11682 (2014).
- Slater M D, Kim D H, Lee E, et al. *Sodium-ion batteries*. Advanced Functional Materials, **23**, 947-958 (2013).
- Saiful Islam M, Fisher-Craig A J. *Lithium and sodium battery cathode materials: Computational insights into voltage, diffusion and nanostructural properties*, Chemical Society Reviews, **43**, 185-204 (2014).
- Chevrier V. L., Ceder G. *Challenges for Na-ion negative electrodes batteries and energy storage*. Journal of the Electrochemistry Society, **158**, A1011-A1014 (2011).
- Zaghib K., Trottier J., Hovington P., et al. *Characterization of Na-based phosphate as electrode materials for electrochemical cells*. Journal of Power Sources, **196**, 9612-9617 (2011).
- Zheng Y., Zhang P., Wu S. Q., et al. *First-principles investigations on the $\text{Na}_2\text{MnPO}_4\text{F}$ as a cathode material for Na-ion batteries*, Journal of the Electrochemistry Society, **160**, A927-A932 (2013).
- Recham N., Chotard J. N., Dupont L., et al. *Ionothermal synthesis of sodium-based fluorophosphate cathode materials*, Journal of the Electrochemistry Society, **156**, A993-A999 (2009).

8. Tepavcevic S., Xiong H., R. Stamenkovic V. R., et al. *Nanostructured bilayered vanadium oxide electrodes for rechargeable sodium-ion batteries*, ACS Nano, **6(1)**, 530-538 (2012).
9. Jian Z. L., Zhao L., Chen W., et al. *Carbon coated $Na_3V_2(PO_4)_3$ as novel electrode material for sodium ion batteries*, Electrochemistry Communications, **14**, 86-89 (2012).
10. Brian L. Ellis, Linda F. Nazar. *Sodium and sodium-ion energy storage batteries*, Solid State and Materials Science, **16**, 168-177 (2012).
11. Shirakawa J., Nakaya M., Wakihar M., et al. *Changes in electronic structure upon lithium insertion into $Fe_2(SO_4)_3$ and $Fe_2(MoO_4)_3$ investigated by X-ray absorption spectroscopy*, Journal of Physical Chemistry B, **11**, 1424-1430 (2007).
12. Nguyen V T, Liu Y L, Chen W, et al. *Synthesis and electrochemical performance of $Fe_2(MoO_4)_3$ /carbon nanotubes nanocomposite cathode material for sodium-ion battery*, ECS Journal of Solid State Science and Technology, **4(5)**, M25-M29 (2015).

Corresponding author: **Nguyen Van Tu**

Institute for Chemistry and Materials
Military Institute of Science and Technology
17, Hoang Sam, Nghia Do, Cau Giay, Hanoi, Vietnam
E-mail: nguyenvantu882008@yahoo.com.